Topical Review

Synchrotron-Based X-Ray Fluorescence Microscopy as a Technique for Imaging of Elements in Plants[1][OPEN]

Peter M. Kopittke,[a] Tracy Punshon,[b] David J. Paterson,[c] Ryan V. Tappero,[d] Peng Wang,[e,f,2] F. Pax C. Blamey,[a] Antony van der Ent,[g] and Enzo Lombi[h,3]

[a]University of Queensland, School of Agriculture and Food Sciences, St. Lucia, Queensland 4072, Australia
[b]Dartmouth College, Department of Biological Sciences, Life Science Center, Hanover, New Hampshire 03755
[c]Australian Synchrotron, Clayton, Victoria 3168, Australia
[d]Brookhaven National Laboratory, Photon Sciences Division, Upton, New York 11973
[e]Nanjing Agricultural University, College of Resources and Environmental Sciences, Nanjing 210095, China
[f]University of Queensland, Centre for Soil and Environmental Research, School of Agriculture and Food Sciences, St. Lucia, Queensland 4072, Australia
[g]University of Queensland, Centre for Mined Land Rehabilitation, Sustainable Minerals Institute, St. Lucia, Queensland 4072, Australia
[h]University of South Australia, Future Industries Institute, Mawson Lakes, South Australia 5095, Australia

ORCID IDs: 0000-0003-4948-1880 (P.M.K.); 0000-0003-0409-9012 (D.J.P.); 0000-0002-3560-2461 (R.V.T.); 0000-0001-8622-8767 (P.W.); 0000-0002-6492-1939 (F.P.C.B.)

Understanding the distribution of elements within plant tissues is important across a range of fields in plant science. In this review, we examine synchrotron-based x-ray fluorescence microscopy (XFM) as an elemental imaging technique in plant sciences, considering both its historical and current uses as well as discussing emerging approaches. XFM offers several unique capabilities of interest to plant scientists, including in vivo analyses at room temperature and pressure, good detection limits (approximately 1–100 mg kg^{-1}), and excellent resolution (down to 50 nm). This has permitted its use in a range of studies, including for functional characterization in molecular biology, examining the distribution of nutrients in food products, understanding the movement of foliar fertilizers, investigating the behavior of engineered nanoparticles, elucidating the toxic effects of metal(loid)s in agronomic plant species, and studying the unique properties of hyperaccumulating plants. We anticipate that continuing technological advances at XFM beamlines also will provide new opportunities moving into the future, such as for high-throughput screening in molecular biology, the use of exotic metal tags for protein localization, and enabling time-resolved, in vivo analyses of living plants. By examining current and potential future applications, we hope to encourage further XFM studies in plant sciences by highlighting the versatility of this approach.

The distribution and concentration of elements, both essential and nonessential, within plant tissues change over time in response to physiological stimuli, developmental stage, and the external environment. To improve the understanding of genetic and physiological processes controlling plant growth, it is necessary to understand these changes both statically and dynamically at the tissue, cellular, and subcellular levels. The distribution of elements within plant tissues is informative for studies ranging from functional characterization in molecular biology, improving human nutrition, improving plant health and climate adaptability, to the movement and toxicity of contaminants throughout the food chain.

The range of methods suitable for examining the concentration and distribution of elements within plants includes x-ray fluorescence microscopy (XFM), scanning electron microscopy coupled with energy-dispersive x-ray spectroscopy, nanoscale secondary ion mass spectrometry, laser ablation inductively coupled plasma mass spectrometry (LA-ICP-MS), microparticle-induced x-ray emission, confocal microscopy with fluorophores, and autoradiography with radioactive isotopes. These various techniques all have advantages and disadvantages, differing not only in the extent of sample preparation required but also in sensitivity (detection limit), resolution, detectable elements, and probed volume (Lombi et al., 2011b). Of particular

[1]Much of this research was undertaken on the x-ray fluorescence microscopy beamline at the Australian Synchrotron, part of the Australian Nuclear Science and Technology Organisation. P.W. would like to thank the support by National Key Research and Development Program of China (2016YFD08004002). A.v.d.E. is the recipient of a Discovery Early Career Researcher Award (DE160100429) from the Australian Research Council. Parts of this research used the XFM Beamline of the National Synchrotron Light Source II, a U.S. Department of Energy (DOE) Office of Science User Facility operated for the DOE Office of Science by Brookhaven National Laboratory under Contract No. DE-SC0012704.

[2]Author for contact: p.wang3@njau.edu.cn.
[3]Senior author.

P.M.K. developed the ideas and prepared the initial framework; the manuscript was written by P.M.K., T.P., D.J.P., R.V.T, P.W., F.P.C.B., A.v.d.E., and E.L.

[OPEN]Articles can be viewed without a subscription.
www.plantphysiol.org/cgi/doi/10.1104/pp.18.00759

ADVANCES

- XFM techniques are evolving more rapidly than other approaches, allowing for in vivo analyses of metal(loid)s in biological tissues at room temperature and pressure, with low detection limits, excellent resolution, and no theoretical restrictions on sample size.
- The recent development of faster fluorescence detector systems and control systems allow routine scanning with dwell times ≤1 ms, with this being 10,000-fold faster than two decades ago.
- These advances have allowed for implementation of new approaches across the plant sciences, including for functional characterization with molecular biology, examining the distribution of nutrients in human food, understanding the efficacy of foliar fertilizers, investigating engineered nanoparticles, and examining the distribution and concentration of metal(loid)s in agronomic and hyperaccumulating plant species.

interest in this study is XFM, which offers several unique capabilities, including allowing for in vivo analyses at room temperature and pressure, providing good detection limits (approximately 1–100 mg kg^{-1}) and an excellent resolution (down to 50 nm), and having no theoretical restrictions on sample size (some XFM beamlines are able to analyze objects with dimensions greater than 1 m). We would argue that the pace at which XFM techniques have evolved over the past two decades is substantially faster than the progress made in many other instrumentation areas and will continue to provide new capabilities in the future.

Although XFM can be either synchrotron based or benchtop based, the focus of this review is on synchrotron-based approaches, because they have several advantages (e.g. including a photon flux that is orders of magnitude higher). As a result, synchrotron-based XFM analyses are typically orders of magnitude faster than benchtop systems, which is critical for the analysis of hydrated plant tissues (for an example of plant analyses using a benchtop-based system, see Fittschen et al., 2017). Despite its advantages, synchrotron-based XFM analysis remains a comparatively little-utilized approach within plant sciences.

The aim of this review is to (1) briefly describe the theory of synchrotron-based XFM, (2) review its historical and current uses within the plant sciences, and (3) discuss emerging XFM approaches and their implications. This review builds upon the early reviews by Schulze and Bertsch (1995) and Bertsch and Hunter (2001) as well as those that are more recent, including Punshon et al. (2009), Lombi et al. (2011b), Zhao et al. (2014), Castillo-Michel et al. (2017), and van der Ent et al. (2018). It is our aim to encourage studies by highlighting the versatility of XFM analyses and by examining recent technological improvements that provide new opportunities.

SYNCHROTRON RADIATION

Introduction to Synchrotron Radiation

Synchrotrons generally consist of a linear accelerator, a booster ring, a storage ring, and a number of beamlines, or experimental end stations where the photons (often an x-ray beam) and the sample meet. In the linear accelerator, an electron gun fires electrons, which, by the time they reach the end of the linear accelerator, are traveling at almost the speed of light. The electrons then enter a booster ring, where they are rapidly accelerated even further. Electrons then enter the storage ring, which circulates the electrons in a nearly circular ring for as long as possible. In the storage ring, bending magnets and insertion devices (wigglers and undulators) bend (accelerate) the electron path, resulting in the production of photons (synchrotron light). These photons vary in energy, typically from approximately 10^{-3} to 10^{5} eV (infrared to hard x-rays) as a function of how they are produced.

The photons travel at a tangent to the storage ring, into experimental end stations, where the synchrotron light is brought onto the sample. Experiments depend not only upon the energy of the photons (infrared, soft x-rays, hard x-rays) but also upon the techniques used. Although similar to photons produced by benchtop sources, synchrotron-produced photon beams have several advantages: they are extremely bright (shortening per-pixel dwell times and allowing faster analysis), monochromatic (making robust quantification possible), and tuneable (enabling x-ray absorption spectroscopy to probe chemical speciation).

XFM Beamlines

At an XFM beamline, the x-rays from the storage ring first pass through a monochromator, which is used to select those of specific energies. The x-ray beam is then focused onto the sample, with spot sizes typically ranging from 1 to 10 µm for a microprobe and 50 to 500 nm for a nanoprobe. The sample is then scanned through the beam in a raster pattern to produce elemental maps based upon the characteristic fluorescent x-rays emitted (photoelectric effect) at each part of the sample (for a discussion of the photoelectric effect in a biological context, see Lombi and Susini, 2009). Fluorescent x-rays are quantified using a detector, located either perpendicular to the incident x-ray beam or in a backscatter geometry. Accessible elements depend

upon the configuration and capabilities of the beamline and the energy selected, but they often range from approximately 2 to 25 keV, or P to Ag at their K edges and higher Z-elements at the L edges. Soft x-ray imaging is not considered here but can be used for lighter elements in plant tissues, such as Na, Si, O, or Al (Tolrà et al., 2011). We do not consider soft x-ray imaging in this review because analyses must be done in a vacuum; hence, hydrated tissues and living plants cannot be examined, and most samples must typically be dehydrated, resin embedded, and sectioned.

New-generation fast detector systems (see "Current Applications of Element Imaging in Plants"), such as the Maia detector system comprising an array of 384 detectors, can process photon rates exceeding 10^7 s^{-1} (Ryan et al., 2010). This results in pixel transit times as short as 50 µs, which enables the production of megapixel elemental maps in a short time. The Maia detector system is currently implemented at four facilities: the Australian Synchrotron, in the United States (Advanced Photon Source and Cornell High Energy Synchrotron Source), and in Germany (Deutsches Elektronen-Synchrotron). Other synchrotron XFM beamlines typically use silicon drift detectors, which are increasingly also exploiting the advantages of fast electronics and also are able to attain transit times per pixel in the millisecond range.

EARLY STUDIES EXAMINING ELEMENT DISTRIBUTION IN PLANT TISSUES

Synchrotrons were first used in plant analysis in the 1990s. Applications included tree ring analysis (Gilfrich et al., 1991; Berglund et al., 1999), because wood has an accretionary growth form that can contain a record of metal exposures. In other early studies, roots of *Plantago lanceolata* and a living leaf of *Lotus corniculatus* were imaged (Yun et al., 1998; Fukumoto et al., 1999). These early studies were essentially a proof of concept rather than an attempt to address specific scientific questions. Indeed, by current standards, these studies were hindered by the inefficiency of the fluorescence detectors, which resulted in a poor detection limit per unit dwell, and hence long periods of time were required to collect maps. For example, in the study of Berglund et al. (1999), the dwell was 10 s $pixel^{-1}$, which, for their map of 204 × 92 pixels, would have taken approximately 52 h to collect.

As a result of inefficient fluorescence detectors and long scan durations, early studies lacked replication, were confined to a limited number of treatments, required the sample to be stable (i.e. dehydrated), and generally examined only small sample areas at low resolution. Another implication was that studies tended to focus largely on hyperaccumulator plants (Reeves et al., 2018), because the high concentrations of elements in these plant species were easier to measure. The utility of XFM in plant sciences became apparent from these early studies (Pickering et al., 2000, 2006; Scheckel et al., 2004, 2007; McNear et al., 2005; Freeman et al., 2006; Tappero et al., 2007).

Of the early XFM studies, few examined the element distribution in plant species of agronomic interest, due to their relatively low element concentrations. This pioneering early work almost certainly served as a catalyst for technological advances that would ultimately bring economically important crop plant species within the reach of XFM analysis. These included examination of Zn in tomato (*Solanum lycopersicum*) roots infected with mycorrhizae (Sarret et al., 2003), Zn in roots, petioles, and leaves of rocket (*Eruca vesicaria*; Terzano et al., 2008), Se in the roots of onion (*Allium cepa*; Bulska et al., 2006), and metal(loid) distribution in rice (*Oryza sativa*) grains (Meharg et al., 2008; Takahashi et al., 2009). Finally, in an elegant study of Fe distribution in intact seeds of Arabidopsis (*Arabidopsis thaliana*), Kim et al. (2006) identified the role of the vacuolar membrane transporter VIT1 in Fe loading in seeds, with their findings being relevant for Fe biofortification of seeds.

CURRENT APPLICATIONS OF ELEMENT IMAGING IN PLANTS

In the last decade, numerous technological advances made XFM a critical analytical technique in plant science. Faster fluorescence detector systems, focusing optics, motion-control systems, encoding, and electronics have allowed routine scanning with dwell times of 1 ms or less. This is at least 10,000-fold faster than in the study of Berglund et al. (1999) and about 1,000-fold faster than in most studies conducted in the first decade of this century (Supplemental Fig. S1). Fast scanning allowed appropriate biological replication, larger scan areas, and, critically, the examination of hydrated specimens in two and three dimensions. With the new generation of fast and efficient fluorescence detector systems, we will now examine the interlinked current applications for XFM within a range of plant science fields.

Functional Characterization with Molecular Plant Biology

Studies linking the elemental imaging capabilities of XFM with genetic approaches offer marked opportunities for the examination of gene × environment interactions in planta. Such approaches are of particular interest in characterizing genes that regulate elemental homeostasis in plants, for example by comparing transporter phenotypes, without the need to resort to gene expression in model organisms. This information is important across a wide range of applications, yet comparatively few studies have utilized XFM for this approach (Donner et al., 2012).

Most studies that have used XFM for functional characterization with molecular plant biology have focused on understanding the processes controlling micronutrient concentrations required for the biofortification

of food products. Kim et al. (2006) examined changes in Fe distribution following silencing of the gene responsible for a vacuolar membrane transport protein in Arabidopsis seeds, using microtomography to generate three-dimensional images of Fe. Also using Arabidopsis, Chu et al. (2017) found that METAL TOLERANCE PROTEIN8 (MTP8) determined the distribution of Fe and Mn in seeds. Using XFM in Arabidopsis circumvented the methodological challenges of GFP imaging in quiescent seed tissue while also providing functional information in vivo. XFM analysis is more efficient for Arabidopsis seeds (size, approximately 300 µm × 900 µm) than for the seeds of model plants such as rice. Zhai et al. (2014) examined the role of OPT3 in phloem-specific loading of Fe, Eroglu et al. (2017) examined the role of MTP8 in the transport of Mn across the tonoplast, and Conte et al. (2013) examined changes in Fe distribution in seeds in the double loss-of-function mutant *ysl1ysl3*. Furthermore, Johnson et al. (2011) examined the role of overexpressing the *NAS* gene family in rice, focusing on changes in Fe and Zn in the grain and the relationships between these two micronutrients in the endosperm with phytic acid, an important antinutrient that limits the absorption of Fe in the human digestive system.

In addition to changes in micronutrient distribution for biofortification, XFM combined with plant molecular genetics has been applied to macronutrients. XFM mapping was used to show the differences in Ca localization and speciation in a *calcium oxalate deficient5* (*cod5*) mutant of *Medicago truncatula* (Punshon et al., 2013). Oxalate influences Ca bioavailability, with crucial roles in plant defense, rigidity, detoxification, and light gathering. Deleting *COD5* altered both Ca distribution and the form of Ca oxalate, preventing biogenic crystal formation. Calcium endomembrane transporter proteins (CAXs), which transport Ca^{2+} among other cations, were analyzed in Arabidopsis (Punshon et al., 2012). Using *cax1* and *cax3* loss-of-function lines as well as lines expressing deregulated CAX1, these authors identified cell type-specific functions of *CAX1* and *CAX3* for the partitioning of Ca into organelles. Finally, Chao et al. (2014) used XFM to examine the distribution of a contaminant, As, in Arabidopsis, identifying a new arsenate reductase enzyme that limits As accumulation in plant tissues.

The common feature in most of the studies mentioned above is that they characterized the functions of membrane-bound element transport protein systems; disruption (e.g. mutagenization or overexpression) of these proteins can cause substantial elemental redistribution phenotypes. Furthermore, the location of the elemental phenotype corresponded to the tissues in which genes encoding for the proteins were differentially expressed.

Distribution of Nutrients within Foods for Human Nutrition

Biofortification is the development, via traditional breeding or genetic manipulation, of food crops with enhanced concentrations or bioavailable essential nutrients. Understanding the concentration and distribution of nutrients in food products is essential for this effort. For example, one of the most common human and animal dietary health problems is Fe deficiency, with 2 billion people worldwide anemic (WHO, 2007). Similarly, an estimated 31% of the global human population suffers from Zn deficiency, causing a loss of 28 million life-years annually (Caulfield and Black, 2004), with most depending upon cereal grains and legumes as their primary dietary source of Zn (Myers et al., 2014) and source of calories.

For biofortification, nutrient distribution and bioavailability are as important as concentration. In cereal grains, such as wheat (*Triticum aestivum*) and rice, milling to produce white flour or rice removes the bran layers and the embryo, in which the mineral nutrients are located almost exclusively (see below). The distribution of nutrients within the various tissues of the grain will influence the nutritional value, and biofortification strategies need to consider nutrient distribution to ensure their success (Fig. 1A). For wheat and rice, the majority of micronutrients are located in the bran layers (aleurone, tegument, and pericarp), with the elements mobile in the xylem (Mn, Si, Ca, and Sr) found in the outermost bran layer and elements mobile in the phloem (K, Mg, P, Fe, Zn, and Cu) more concentrated in the aleurone layer (De Brier et al., 2015). Another area of micronutrient enrichment (e.g. Fe and Zn) is located in the embryo and crease tissues (Neal et al., 2013; Ajiboye et al., 2015; De Brier et al., 2016; Ramos et al., 2016), with concentrations in the endosperm being markedly lower. The colocalization of Zn and especially Fe with P is an indication of complexation of these micronutrients by phytate (inositol 6-hexakisphosphate), greatly reducing their bioavailability. High-resolution XFM analyses of whole grains has shown that, in the embryo and the nucellar projection, for instance, Zn and Fe are not colocalized with P and may have increased bioavailability (Neal et al., 2013; De Brier et al., 2016). The steep gradient in concentration between micronutrients in the outer part of the grains means that milling strategies can be tailored to maximize the nutritional value of milling products. Practices such as pearling (the removal of the outer part of the grains by abrasion) before milling can be used to produce raw materials of improved nutritional quality (De Brier et al., 2015). Similar results also have been reported for barley (*Hordeum vulgare*) and rice (Takahashi et al., 2009; Lombi et al., 2011c; Kyriacou et al., 2014), with concentrations highest in the embryo, crease, and outer tissues, being at least 1 order of magnitude lower in the endosperm. In rice, while Fe generally is present in phytate granules in the aleurone layer, a fraction of this micronutrient also is present in the subaleurone and outer endosperm (Kyriacou et al., 2014). XFM also has been used to investigate the redistribution of elements during germination and as a

consequence of parboiling (Takahashi et al., 2009; Oli et al., 2016). Finally, XFM also can be used to examine how various biofortification approaches (such as foliar fertilization) influence the concentrations and distributions of nutrients within the grain (Ajiboye et al., 2015; Ramos et al., 2016; Zhang et al., 2018).

Foliar Fertilizers

The application of foliar fertilizers is particularly useful in areas where soil-based applications of nutrients are ineffective (e.g. application of Zn fertilizers to alkaline soils). However, the mechanisms governing the movement of foliar-applied nutrients across the leaf surface and translocation throughout the plant are poorly understood (Fernández and Brown, 2013).

Increasingly, XFM approaches have been used to study the distribution of foliar-applied Zn within plant tissues (Fig. 2). XFM was used to compare the transport of different forms of foliar-applied Zn (including $ZnSO_4$ and Zn-EDTA) in the phloem within the petioles of sunflower (*Helianthus annuus*), and the extent of Zn mobilization following absorption influenced its efficacy (Tian et al., 2015). While volume-averaged elemental analyses (ICP-MS) were unable to detect an enhanced concentration of Zn in treated sunflower petioles (probably due to the high Zn background concentration), a clear enrichment of Zn in the vascular tissues of treated plants was detected by XFM (Tian et al., 2015). Foliar absorption of Zn was found to increase concentrations in the leaf tissues directly underlying the applied Zn, with concentrations increasing up to 600-fold in tomato but only 5-fold in the waxy leaves of citrus (*Citrus reticulatus*; Du et al., 2015). However, once the Zn had moved across the leaf surface, it appeared to bind strongly with only limited translocation, with tissue Zn concentrations decreasing rapidly to background levels at a distance of only 1 to 10 mm from the site of application (Du et al., 2015). Foliar absorption of Zn, Fe, and Mn in the leaves of tomato, sunflower, and soybean (*Glycine max*) had a similar outcome (Li et al., 2017). To understand the route (e.g. via the cuticle, stomata, or trichomes; for details, see Fernández and Brown, 2013) of foliar-applied Zn movement across the leaf surface, Li et al. (2018a) used XFM to examine both intact leaves and leaf cross sections of soybean and tomato. While some Zn accumulated in the trichomes, this was not the major pathway for the movement of Zn across the surfaces of leaves in these two plant species. Unlike for soybean and tomato, for the leaves of sunflower, trichomes were found to be an important pathway for the rapid movement of foliar-applied Zn (Li et al., 2018).

Engineered Nanoparticles

Engineered nanoparticles (NPs), defined as particles between 1 and 100 nm in size, possess unique physicochemical properties that differ from those of their molecular and bulk counterparts. These materials are being used increasingly in a wide range of consumer products, such as sunscreens, hair-restorative shampoos, and a wide range of antibacterial products. With little regulation, their release into the environment is largely unavoidable. Furthermore, NPs also have been developed as effective delivery tools with numerous applications in human systems for targeted drug delivery, cancer therapy, and treatment for loss-of-function genetic disease (Wang et al., 2016). This could potentially allow for the development of smart crops, such as NP-mediated, targeted delivery of agrochemicals, bioactive molecules, and molecular markers (Wang et al., 2016; Mitter et al., 2017). Although these applications in plant sciences are promising, little is known about the interactions between plants and NPs and the subsequent uptake and targeted translocation of NPs in planta.

The methodology for the use of XFM in the analysis of NPs in plants was reviewed recently by Castillo-Michel et al. (2017). XFM has been used to examine the distribution of a range of NPs in plant tissues, including Ag-NPs (Larue et al., 2016; Martínez-Criado et al., 2016; Wang et al., 2017), CeO_2-NPs (Hernandez-Viezcas et al., 2013; Zhao et al., 2015; Ma et al., 2017; Spielman-Sun et al., 2017), TiO_2-NPs (Servin et al., 2012; Larue et al., 2016), and ZnO-NPs (Hernandez-Viezcas et al., 2013; Wang et al., 2013b; Zhao et al., 2015). Overall, NPs can potentially be taken up by plants and translocated from roots to shoots (see Wang et al. [2017] for Ag and Ma et al. [2017] for Ce). Interestingly, Spielman-Sun et al. (2017) were able to show how NP surface charge could modify the root interaction and the leaf distribution of CeO_2, with negatively charged NPs interacting less with the root surface but having higher mobility within the plant than neutral and positively charged NPs of the same size. However, unfortunately, the resolving power of most XFM analyses makes the analysis of individual NPs challenging. As improved x-ray optics are developed, nano-XFM is becoming possible and new systems will enable analyses with resolution down to the tens of nanometers (Castillo-Michel et al., 2017). For example, nanoscale resolution has been used to examine the distribution of Ag-NPs inside a human monocyte (Wang et al., 2015a) and the vascular bundles and Casparian strip of a sunflower root (Martínez-Criado et al., 2016). These advances in resolution will undoubtedly facilitate breakthroughs in the study of plant-NP interactions.

Metal(loid) Toxicity in Agronomic Plant Species

Over the last decade, interest in the distribution of toxic metals in crop plants has increased considerably. Some metals are toxic because they directly reduce plant growth, while other metals accumulate to levels within the plant tissues that are toxic to animals (including humans) but not to the plant itself. For the former

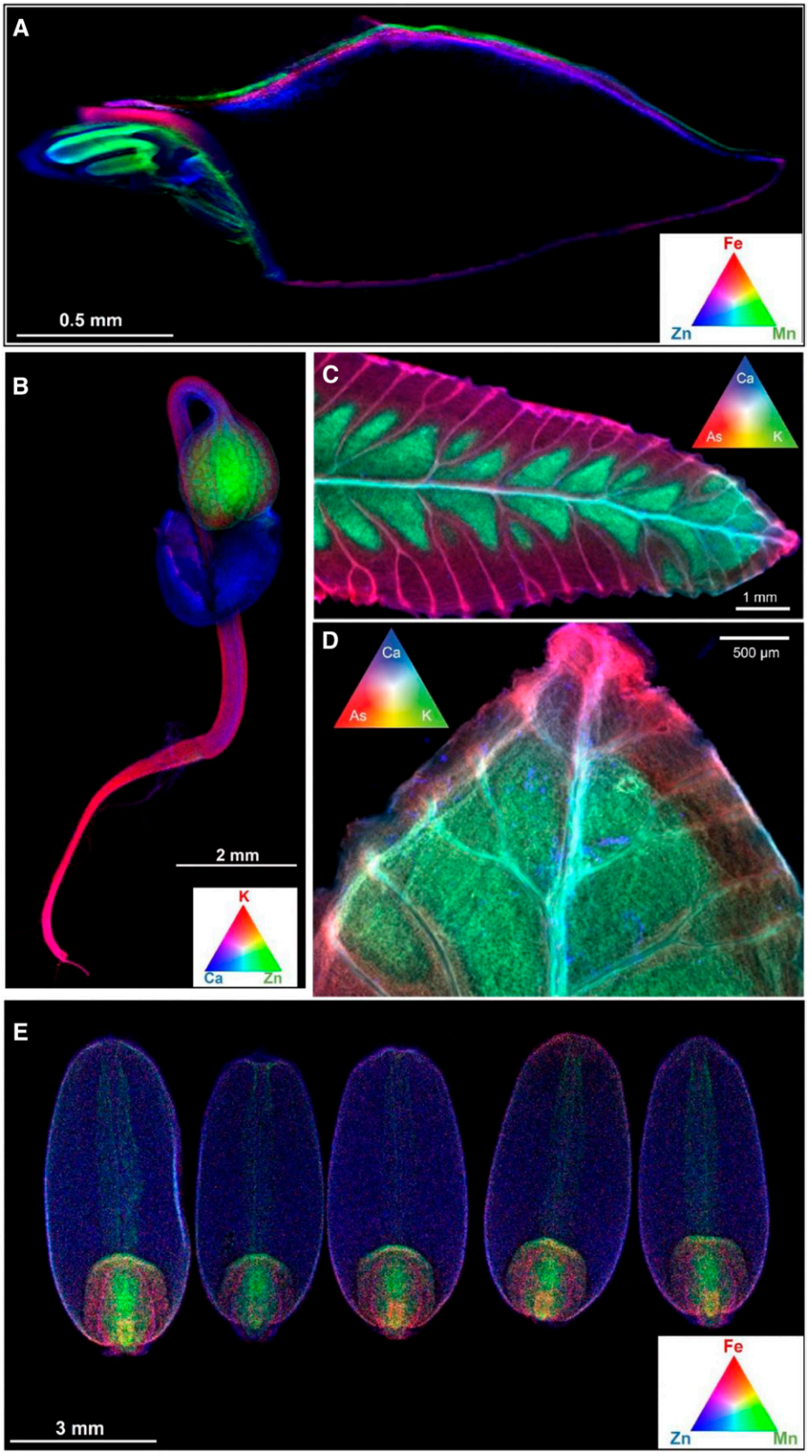

Figure 1. Distribution of nutrients in plant tissues examined using XFM. A, Tricolor image showing Fe, Mn, and Zn distribution in a longitudinal section (70 µm thick) of a barley grain. The original scan was 2,320 × 880 pixels (approximately 2 megapixels) with a pixel transit time of approximately 0.6 ms, resulting in a scan duration of approximately 20 min (Lombi et al., 2011c). B, Image from XFM analyses of a scan of a living seedling of *Noccaea caerulescens* (a hyperaccumulator) showing Zn (green),

(i.e. for elements for which their toxicity reduces crop yield), the interest is generally in understanding the phytotoxicity mechanisms (Fig. 3). An example of this is Mn, concentrations of which increase markedly in acid and waterlogged soils. In leaves of soybean, sunflower, white lupin (*Lupinus albus*), and narrow-leafed lupin (*Lupin angustifolius*), differences in Mn tolerance could be ascribed to variations in Mn distribution and speciation (Blamey et al., 2015). Specifically, the sensitivity of soybean to high Mn was due to a lack of an effective Mn sink, such as trichomes or vacuoles. Alleviation of Mn toxicity is afforded by Si, which binds Mn within the cell wall, presumably constituting a detoxification mechanism (Blamey et al., 2018a). The toxic mechanisms of Cu, Zn, Ni, and Mn were examined in roots of cowpea (*Vigna unguiculata*; Kopittke et al., 2011, 2013) and that of Cu was examined in rice (Lu et al., 2017), showing that Cu rapidly binds strongly to the cell walls of the outer tissues of the root cylinder (rhizodermis and outer cortex), where it inhibits wall loosening as required for cell elongation.

Reducing the amount of certain potentially toxic metal(loid)s within the edible portion of the plant in order to improve food safety also is a priority. Of particular concern is As, a known human carcinogen that accumulates within rice grain, a staple food eaten by approximately half of the global population on a daily basis. This poses a health risk to populations with a high rice consumption (Melkonian et al., 2013), particularly those who also live in areas where groundwater As contamination also is an issue. Of critical importance is determining the route that As takes through the plant, and XFM analysis has been instrumental in resolving this (Kopittke et al., 2012, 2014). XFM also has shed light on how As is distributed within the rice grain itself (Meharg et al., 2008; Lombi et al., 2009), information that is used directly by many human health scientific disciplines to establish risk and advocate for the regulation of As in food. In a similar manner, there is increasing concern regarding the accumulation of Cd within rice grain, particularly in Asia (Song et al., 2017). We are aware of only two studies using XFM to examine the distribution of Cd in rice, with Yamaoka et al. (2010) examining its distribution in the stem (where it accumulated within the vascular tissues) but not in the grain itself and with Meharg et al. (2008) examining Cd distribution in rice grain.

Metal(loid)s in Hyperaccumulators

Hyperaccumulators are plants that accumulate metal(loid)s to concentrations thousands of times higher than most other plant species (Reeves et al., 2018). The elements As, Cd, Mn, Ni, Zn, and Se can be accumulated either singly or in combination with other elements by hyperaccumulators (Fig. 1B). Knowing how these hypertolerance and sequestration mechanisms operate is valuable information for soil remediation. Synchrotron-based XFM has had a key role in answering questions regarding metal(loid) regulation in plants, from the rhizosphere to uptake pathways in the roots and translocation through the shoot. One of the most intensively studied elements is Se in *Astragalus bisulcatus* and *Stanleya pinnata*, including using both XFM elemental mapping and chemical speciation mapping (Pickering et al., 2000; Freeman et al., 2006; Valdez Barillas et al., 2012). These studies have shown that Se is taken up mainly as selenate, whereas, in the plant tissues, Se occurs predominantly in organo-Se compounds such as methyl-SeCys and also *C*-glutamyl-methyl-SeCys (*A. bisulcatus*) or selenocystathionine (*S. pinnata*). Se is stored mainly in the epidermis and trichomes in these species, presumably isolated from sensitive cellular machinery. Trichomes are hairs on the leaf surface, and storage of potentially toxic metals in trichomes under conditions of excess has been a frequent observation of both hyperaccumulators and other plant species (for discussion, see Blamey et al., 2015). Trichomes may have an evolutionary role in discouraging herbivory (Werker, 2000), and their use to store potential toxins is consistent with that hypothesis.

Fluorescence and absorption-edge computed tomography and micro-x-ray absorption spectroscopy (micro-XAS), complementary synchrotron-based techniques that are used to probe the coordination state and nearest neighbor identity of elements (Lombi and Susini, 2009), were used to probe Ni in *Alyssum murale* (McNear et al., 2005). This revealed Ni accumulation in the stem and leaf epidermis, colocalized with Mn in trichome bases. Ni was complexed mainly with malate and other carboxylic acids. X-ray absorption-edge computed tomography and micro-XAS also has been used for speciation imaging of Tl in *Iberis intermedia* (Scheckel et al., 2004, 2007), with Tl(I) present as the aqueous species with the highest concentrations in the leaf veins. Chemical speciation mapping has been used for localizing the chemical transformations of As in *Pteris vittata*, which revealed that arsenate is transported through the vascular tissue from the roots to the fronds, where it is reduced to arsenite (Pickering et al., 2006). Furthermore, XFM analysis showed that As is localized on the pinna surface in the proximity of veins (Fig. 1, C and D) and is present especially in the apoplast (Datta et al., 2017). Speciation imaging techniques have numerous potential applications in plants, but their greatest utility is in situations where different

Figure 1. (*Continued.*)
K (red), and Ca (blue). Data are from A. van der Ent (unpublished). C and D, Images from XFM analyses of scans of a leaflet of *P. vittata* (an As hyperaccumulator) showing K (green), As (red), and Ca (blue). Data are from R.V. Tappero (unpublished). E, An initial attempt using XFM to rapidly scan whole and intact wheat seeds (cv Shield). The transit per 20-μm pixel was 15 mm s^{-1} velocity, with the entire scan duration being approximately 8 min. Data are from E. Lombi (unpublished).

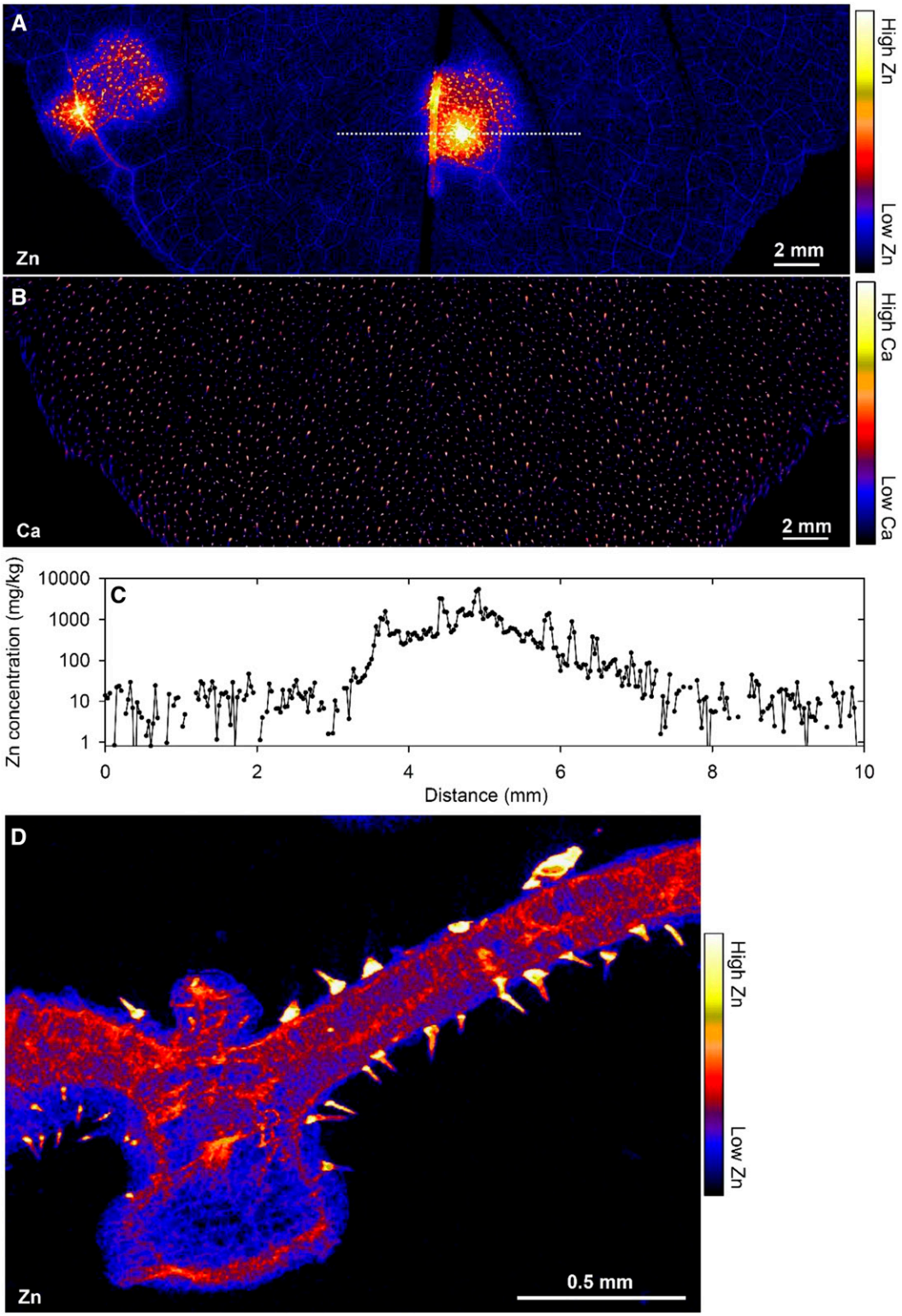

Figure 2. Distribution of nutrients in leaf tissues of sunflower examined using XFM following foliar fertilization with Zn. A and B, Distribution of Zn (A) and Ca (B) in an intact, hydrated leaf of sunflower to which two 5-μL droplets of $ZnSO_4$ (1,000 mg L^{-1} Zn) had been applied on the adaxial surface toward the tip. Note that the highest concentrations of foliar-absorbed Zn accumulated in the trichomes (A), as also can be seen from the high Ca concentrations in these regions (B). C, The concentrations shown for the transect correspond to the dotted white line in A. D, Cross section of a sunflower leaf to which a droplet of $ZnSO_4$ had been applied on the adaxial surface. The entire adaxial area shown was from beneath the droplet.

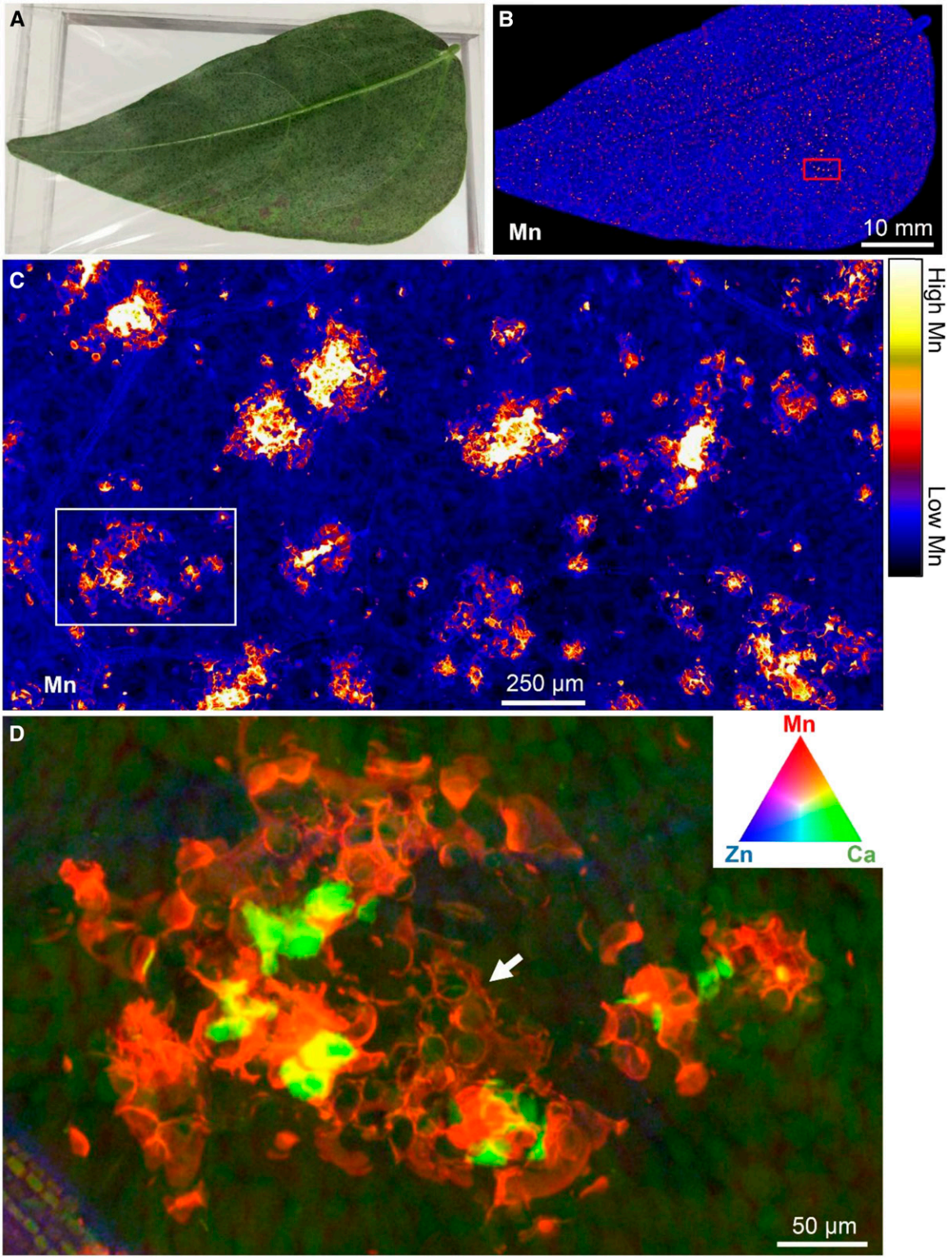

Figure 3. Mn accumulating in an excised (hydrated) trifoliate leaf of cowpea exposed to 30 µM Mn in nutrient solution. A, Image of the leaf. B and C, Distribution of Mn. D, Tricolor image showing Mn, Ca, and Zn. The area scanned in C is indicated by the red rectangle in B, and the area scanned in D is indicated by the white rectangle in C. In D, note how Mn (red) initially accumulates in the cell wall (white arrow), with the green (Ca) circular structures corresponding to vacuoles. For more details and full experimental procedures, see Blamey et al. (2018a).

valence states or binding forms of elements have important ramifications for their toxicity.

In *Arabidopsis halleri*, Cd is complexed mainly with O-ligands and minor S-ligands in the xylem, phloem, mesophyll tissue, and also in the trichomes (Isaure et al., 2015). In *Sedum alfredii*, Zn is associated with malate in the leaves (Lu et al., 2014). In older leaves, Zn is concentrated in the midrib, marginal regions, and the petiole, whereas in young leaves, Zn is distributed uniformly. Further studies also have revealed the chemical speciation and distribution of Cd (Tian et al., 2011) and Pb (Tian et al., 2010) in this plant species.

ADDITIONAL FUTURE STUDIES AND APPROACHES OF VALUE WITHIN PLANT SCIENCES

We now move our discussion from the current plant science applications of XFM to the newly developed (or improved) experimental techniques becoming available at XFM beamlines that open new opportunities to plant scientists. Here, we consider current and anticipated future technological developments expected at XFM beamlines, followed by examples of how emerging techniques can be applied to studies in plant sciences.

Current and Anticipated Future Technological Developments at XFM Beamlines

Four major trends are rapidly changing the landscape for XFM beamlines: (1) better focusing optics; (2) improvements in storage ring design, which result in diffraction-limited storage rings; (3) better and faster detectors for x-ray fluorescence (XRF) detection; and (4) increasing flux.

In general, resolution is improving, especially at next-generation storage rings, which achieve diffraction-limited storage rings, such as at MAXIV (Sweden), with resolution routinely achieved at less than 50 nm. Indeed, advancements in synchrotron emittance and x-ray optics have enhanced focusing capabilities significantly over the last decade by up to 3 orders of magnitude in resolution. The ongoing improvements of Kirkpatrick-Baez mirrors have been revolutionized by the invention of a new polishing technique (e.g. the DESY P06 microprobe [Germany], P10 GINIX [Germany], ID21 and ID16 at ESRF [France], and nanoMAX at MAX IV [Sweden]). Coating mirrors with multilayers allows white or pink beam operation while focusing into the 50-nm range with highest flux. Zone plates also have been improved in structure and especially in thickness for hard x-ray application (Chen et al., 2014). Finally, multilayer Laue lenses have become mature instrumentation for focusing below 20 nm and are being used routinely at the HXN nanoprobe beamline (National Synchrotron Light Source II [United States]).

The development of faster x-ray fluorescence detectors that can routinely acquire at submilliseconds and the combination of large solid angle and on-the-fly detection are resulting in efficient data collection and minimize potential for beam damage. Whereas measurements took seconds of dwell time per image, pixels in past scans are now feasible in the kHz range (Supplemental Fig. S1). The count rate capability was boosted by the introduction of silicon drift detectors and multielement detector arrays (e.g. the Maia detector). Large detection solid angle, on-the-fly scanning mode, and fast data acquisition and processing introduced the third dimension in scanning x-ray fluorescence microscopy (see discussion below).

Among the numerous technological advances that occurred between first- and fourth-generation synchrotron facilities, photon flux (the number of photons striking the sample per unit area) determines both the sensitivity of XFM imaging as well as sample stability. Photon fluxes, within a window that was both high enough to provide sufficient fluorescence of elements at their typical concentration ranges in plant tissues but also low enough to avoid beam damage, was pivotal in opening up the technique to the plant sciences. Researching elemental dynamics in plant tissue requires an avoidance of physical (drying, dehydration) or chemical (infiltration of resins) stabilization, because these processes increase the risk of either movement or changes in elemental speciation. Fluxes on the order of 10^7 to 10^{10} photons s^{-1}, typical of hard x-ray-bending magnet beamlines at second-generation synchrotron facilities, allowed the detection of macronutrients and micronutrients in plants and trace levels of potentially toxic elements such as As with longer dwell times. Now, fluxes have increased through brighter sources and better focusing optics, and fluxes of 10^{11} to 10^{12} photons s^{-1} cause beam damage that can potentially prevent the analysis of fresh or living leaf and root tissue. Although beamlines can take measures to reduce the flux, the magnitude of flux reduction needed to allow fresh plant tissue analysis becomes problematic in fourth-generation synchrotrons, where flux is well over 10^{13} photons s^{-1}. Beam damage can take the form of destruction of tissue and melting of epicuticular waxes, for example. However, it is important to note that concurrent reductions in dwell times, driven by fluorescence detector technologies, from seconds to tens of milliseconds has afforded some solutions, while the advent of fly scanning has largely alleviated this problem. The option to increase spot size, although effective at reducing flux density (especially when higher resolution is not required), has not been available historically but was implemented recently in newly constructed, fourth-generation synchrotrons such as the National Synchrotron Light Source II.

There remain several beamlines equipped for large-scale scanning of whole living plant organs, including BL2-3 at the Stanford Synchrotron Radiation Lightsource (United States), 4-BM at the National Synchrotron Light Source II (United States), and the XFM

beamline at the Australian Synchrotron. Advances in sample preparation, and the provision at many synchrotron facilities of advanced sample preparation equipment and staff, bring in vivo single-cell analysis within the realm of possibility.

These current and anticipated future technological developments will not only enable the further development of studies, as outlined in Section 5, but also permit new studies. We provide examples of such studies and approaches in plant sciences that will be facilitated by ongoing improvements at XFM beamlines.

High-Throughput Screening in Molecular Biology

Elemental uptake, translocation, and storage are under genetic (and environmental) control, being biological functions important for both plant development and human health. However, few genes have been identified due to the lack of efficient methods to screen libraries of mutated plants for individuals that have unusual characteristics in metal metabolism. Although ICP-MS can be used to identify seeds of variants with altered concentrations, this approach is destructive and does not provide laterally resolved information. High-throughput proof-of-concept screening using XFM to examine the distribution of Mn, Fe, Ni, Cu, and Zn in whole, intact seeds of Arabidopsis was conducted over a decade ago (Young et al., 2006). The future use of this approach with new and efficient fluorescence detector systems (Fig. 1E; scanning five wheat seeds required approximately 8 min) would enable orders of magnitude more seeds (and at higher resolution) to be examined.

Use of Exotic Metal Tags for Protein Localization

Immunohistochemistry provides information on the abundance and location of proteins, using either bright-field or fluorescence detection. The use of these chromogenic or fluorescent labels for multiplexed cellular molecular imaging can be difficult for a range of reasons, as would occur, for example, due to overlapping reporter emission spectra. Recently, mass spectrometry immunohistochemistry has been developed, whereby antibodies are labeled with isotopically pure metal chelator tags (Giesen et al., 2014). This approach is useful as it overcomes the problems associated with the spectral overlap of fluorophores. These tags are then liberated from the sample, typically by LA-ICP-MS or laser ablation time of flight mass cytometry (LA-CyToF), allowing up to 40 targets to be examined simultaneously for the visualization of presence, abundance, and location (Levenson et al., 2015). Although LA-ICP-MS and LA-CyToF have been used, XFM also can be used. For example, it would be possible to use the exotic metal tags for simultaneous analyses of nutrient distribution and protein (transporter) localization. Analysis using the metal tags by mass (such as LA-ICP-MS or LA-CyToF) allows the use of isotopes, with Giesen et al. (2014) using a range of isotopes from ^{139}La to ^{176}Yb, for example. In contrast, analysis by XFM would be based upon elemental composition and, hence, would require the use of metals that were not already present at high concentrations within the plant tissues and that also were within the energy range of the beamline. For example, it might be possible to use Ag as a metal tag for XFM analyses.

Time-Resolved, in Vivo Analyses of Living Plants

Fast, two-dimensional XFM imaging now permits time-resolved (kinetic), in vivo, microscopic analyses of element distribution within plants (Fig. 4; Supplemental Figs. S2 and S3). Such an approach would be valuable for numerous studies in plant science, such as those outlined throughout Section 5 of this review, by providing additional information on the kinetic changes in element distribution.

This technique was demonstrated by Blamey et al. (2018b), who examined changes in the distribution of Mn (and other elements) of leaves of cowpea upon exposure to elevated concentrations of Mn in the rooting medium. Repeated XRF scans of leaves of 7-d-old cowpea plants grown in nutrient solutions for 48 h supplemented with Mn showed changes in element concentration and distribution upon exposure to elevated Mn (Supplemental Fig. S3; Blamey et al., 2018b). This repeated XFM scanning did not damage the leaf tissues, due to the rapid speed of scanning (1 ms pixel^{-1}) and the development of an improved scanning approach, which markedly decreased dwell associated with overheads at the end of each horizontal line scan (with this being critical for reducing damage at the edge of the scans). Thus, each of the six scans conducted across the 48-h period took approximately 2 h to complete for an approximately 120-mm^2 area with 4-µm × 4-µm pixels, yielding images of approximately 8.5 megapixels each (Fig. 4; Supplemental Fig. S3).

These time-resolved analyses showed that the accumulation of Mn in spots within the leaf surface was apparent only 12 h after exposure (Fig. 4; Supplemental Fig. S3; Blamey et al., 2018b). Such fully quantitative analyses (Supplemental Fig. S3) permit the calculation, for example, of the rate of change in elemental concentrations for each pixel/region or the calculation of the area with concentrations above a certain threshold. Furthermore, because concentrations of all elements between approximately 2 and 12.9 keV (i.e. P to Se) were measured simultaneously in this particular study, changes in Mn could be related to those in other elements. For example, callose is involved in the expression of Mn toxicity, and the rate of change in Mn concentration (Fig. 4; Supplemental Fig. S3) to that of change in Ca concentration shows that the accumulation of Mn precedes changes in Ca distribution (Fig. 4; Supplemental Fig. S4).

Similarly, Doolette et al. (2018) used this in vivo approach to assess the differential uptake and mobility of Zn supplied as Zn-EDTA or Zn-sulfate by wheat leaves. The same leaves, from plants growing in nutrient

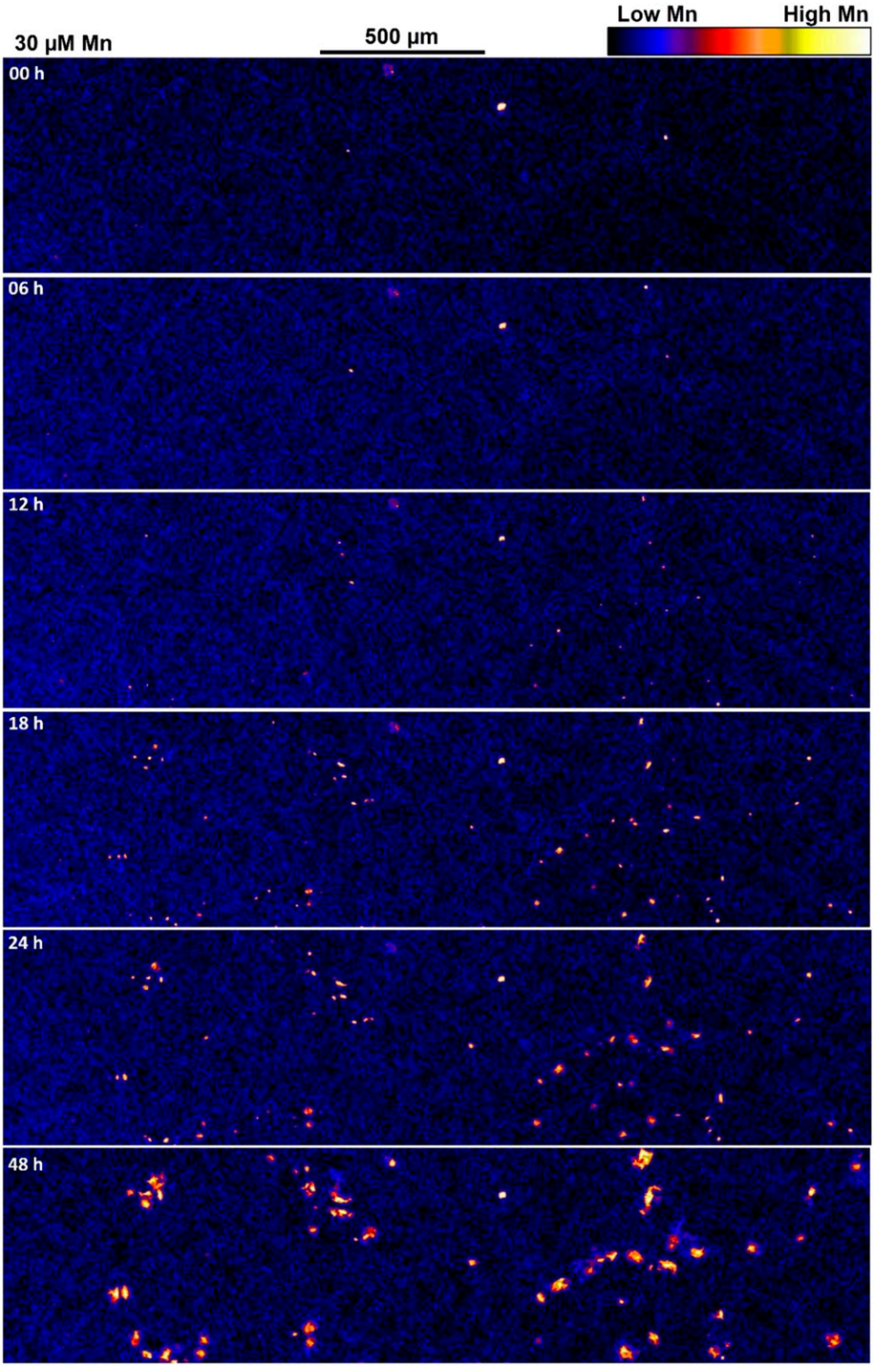

Figure 4. XFM images showing the distribution of Mn in a portion of a cowpea leaf exposed to 30 µM Mn. The area shown here represents only approximately 1.5% of the 8.5-megapixel image obtained for each time interval, which included portions of leaves exposed to both 0.2 and 30 µM Mn. The total area analyzed (i.e. 8.5 megapixels) at each time interval was 120 mm^2, as indicated by the white rectangle in Supplemental Figure S2B. See Blamey et al. (2018b).

solution, were scanned 3, 12, and 24 h after the application of these two fertilizers and revealed that both forms of Zn were taken up readily but that Zn-sulfate was mobilized slightly more than Zn-EDTA from the point of application. Other than those studies listed here, we are unaware of other studies that have provided information on time-resolved analyses in living plants. However, as the resolution at XFM beamlines continues to improve (i.e. better focusing optics), together with faster electronics, in vivo analyses of living plants will become more routine, including for subcellular analyses.

X-Ray Absorption Near-Edge Structure Imaging for Laterally Resolved Speciation

Recently, x-ray absorption near-edge structure (XANES) imaging was developed as a new approach for plant sciences at XFM beamlines (Kopittke et al., 2014; Wang et al., 2015b). To some extent, this approach bridges the gap between imaging (XFM) and speciation (XAS). For instance, a traditional study at an XFM beamline might involve collecting elemental maps before individual XANES spectra (μ-XANES) from points of interest in the map, usually on the basis of contrasting abundance. However, in XANES imaging, it is theoretically possible to extract XANES spectra from every pixel by repeatedly mapping the sample at increasing incident energy across the absorption edge of interest. This approach is similar to that used with *A. bisulcatus* imaged at two energies across the Se edge (Pickering et al., 2000) and in *P. vittata* imaged at three energies across the As edge (Pickering et al., 2006). However, in XANES imaging, it is possible to extract a detailed XANES spectrum for each pixel by repeatedly mapping at many energies (e.g. 100 energies). Again, this approach has been facilitated by the development of fast and efficient fluorescence detectors. For example, in the *A. bisulcatus* example above, the dwell was approximately 5 s pixel^{-1} per energy (Pickering et al., 2000), whereas in the study of Kopittke et al. (2014), the dwell was 4.9 or 9.8 ms pixel^{-1}, yielding a total irradiation time of either 0.4 or 0.8 s pixel^{-1} across the entire XANES stack (81 energy images).

Using laterally resolved data across the root cylinder in wheat and rice, Kopittke et al. (2014) found that As(V) was reduced rapidly to As(III) within the root, with As(V) found only within the rhizodermis. Furthermore, the As(III) was converted rapidly to an As(III)-thiol complex, accounting for all of the As in the cortex and stele. A similar approach was used to show that, in roots and leaves of wheat and rice, selenate was converted efficiently to C-Se-C compounds across the root cylinder, with only 12% to 31% of Se present as uncomplexed selenate in the rhizodermis (Wang et al., 2015b). When exposed to selenite, the Se also was converted efficiently to C-Se-C, with uncomplexed selenite observed only in the outer root tissues. Of interest to biofortification, XANES imaging was used to investigate Fe speciation in wheat grains, which revealed that, while much of the Fe in the aleurone was present as Fe(II) phytate, a portion of the Fe also was bound to nicotianamine in the nucellar projection (De Brier et al., 2016). Finally, XANES imaging also has been used to examine the distribution and speciation of NPs in plant tissues (Castillo-Michel et al., 2017).

One future use of this approach in the plant sciences is to use XFM to screen for differences in elemental speciation between phenotypes. Thus far, genes most amenable to functional characterization via XFM fall into the category of membrane-bound transport proteins, because of their tendency to produce a distributional phenotype when disrupted. With XANES imaging, genes that influence speciation, such as those encoding for ligands or metallochaperones, also could potentially be characterized. In the future, subcellular XANES analyses also would be particularly valuable in understanding differences in speciation within cells.

Microtomography

Due to the penetrating nature of hard x-rays, synchrotron-based x-ray fluorescence microtomography can provide information on the distribution of elements within virtual cross sections of plant tissues with only minor sample preparation (McNear et al., 2005). This is necessary in the many situations in plant science where concentric tissue layers must be distinguished from one another. In these early studies, dehydrated tissues generally were used due to the beam damage associated with the long acquisition times of the scans, but faster, more efficient fluorescence detectors have eliminated this issue (Lombi et al., 2011a), with hydrated roots exposed to environmentally relevant metal concentrations recently becoming amenable to XFM analysis.

Using this approach, Kopittke et al. (2012) obtained virtual cross sections of cowpea roots showing the movement of As through the root cylinder in order to understand uptake and translocation, and Wang et al. (2013a) obtained virtual cross sections of cowpea roots showing the distribution of Se within the root cylinder. Microtomographic analyses also have been used to examine micronutrient distribution within seeds, with Conte et al. (2013) examining the distribution of Fe, Mn, Zn, and Cu in intact seeds of Arabidopsis and in roots and leaves of tomato and cucumber (*Cucumis sativus*; Terzano et al., 2013). Recently, microtomography has been used to examine elemental distribution within an intact leaf of spinifex (*Triodia* spp.; Supplemental Movie S1), with elemental concentrations in the leaf tissue potentially being an indicator for mineral exploration. With ongoing improvements in resolution and in the speed of electronics, subcellular (submicron) three-dimensional tomography will become increasingly available, as demonstrated by de Jonge et al. (2010), who examined elemental distribution in the freshwater diatom *Cyclotella meneghiniana*. However, care must always be taken to avoid damaging the sample during the analysis due to beam damage.

LIMITATIONS

The major limitation for researchers who wish to use synchrotron-based XFM in their experiments is access to synchrotron facilities. There is a need to bridge the gap between what is currently possible in the laboratory and the capability of large facilities. Technological developments, including very-high-flux x-ray sources based on metal jets, and even tabletop accelerators, will not replace synchrotron-based XFM but will permit combining their individual strengths, for example, by whole-plant mapping at the local laboratory followed by targeted investigation at a synchrotron facility (Gei et al., 2018).

Unlike in plant genetics, where submission of raw sequencing data to databases such as GenBank or plantGDB is standard practice (and required by many journals), submission of x-ray spectra into an accessible database is not practiced. The availability of experimental raw data (in a common format) is desirable to have access to as extensive as possible a library of spectra of metal(loid) model components.

As with any approach, where it is not possible to analyze living (hydrated) plant tissues, care must be taken with sample preparation to avoid experimental artifacts (for a discussion of sample-processing approaches, see van der Ent et al., 2018). Furthermore, as discussed above, care must be taken to ensure that the XFM analyses do not cause damage to the sample, resulting, for example, in the potential redistribution of elements (for examples of beam damage caused at XFM beamlines, see the Supplemental Data of Blamey et al. [2018b] and Figure 9 of Lombi et al. [2011b]). In this regard, the use of cryogenic sample preservation during analysis is a potentially useful option to limit sample damage (e.g. mass loss; Beetz and Jacobsen, 2003), particularly when prolonged or repeated analyses are required (such as for tomography or for XANES imaging).

Care also must be taken when comparing the distribution of elements within samples, as the depth within the sample from which different elements can be detected can potentially vary considerably, a problem known as self-absorption. For example, consider a sample of pure water (hydrated plant tissues often are approximately 90% water) that is 0.1 mm thick. For this sample, Zn would largely be detectable throughout the entire sample volume (approximately 7% absorption of Zn K-edge fluorescence at 0.1 mm depth), but P would essentially be undetectable from the deeper portions of the sample (greater than 99% absorption at 0.1 mm depth) due to the lower energy of the fluorescent x-rays for P. In other words, lighter elements tend to be detected preferentially from the shallower portions of samples, while heavier elements are more likely to be detected from within the entire sample depth. Hence, care must be taken when comparing the distribution of elements, particularly for lighter elements.

Finally, in this review, we have focused on XFM as a method for the analysis of element distribution in plant tissue. However, other methods also allow for in situ analyses of element distribution, so care should be taken to select the most appropriate technique. In this regard, Lombi et al. (2011b) and van der Ent et al. (2018) have provided summaries that compare the advantages and disadvantages of various suitable approaches.

CONCLUSION

Overall, this review has examined the use of synchrotron-based XFM in a range of studies in plant sciences, including functional characterization in molecular biology, examining the distribution of nutrients in food products, understanding the movement of foliar fertilizers, investigating engineered NPs, elucidating the toxic effects of metal(loid)s in agronomic plant species, and studying the unique properties of hyperaccumulating plant species. Importantly, we also have identified emerging opportunities (see Outstanding Questions), with these new opportunities being facilitated by the development of new-generation synchrotron facilities, faster fluorescence detector systems, and a range of other beamline improvements. Several key opportunities are identified, such as for high-throughput screening in molecular biology, the use of exotic metal tags for protein localization, and enabling time-resolved, in vivo analyses of living plants (e.g. for kinetic functional characterization in molecular biology). The development and improvement of new techniques at XFM beamlines, such as XANES imaging and microtomography in living plants, also will open new opportunities. It is hoped that this review will encourage further studies that use XFM to examine the distribution and concentration of elements, both essential and nonessential, within plants.

Supplemental Data

The following supplemental materials are available.

Supplemental Figure S1. Relationship between the per-pixel dwell and the time required to complete a nominal one-megapixel scan.

Supplemental Figure S2. Time-resolved, in vivo analyses of living cowpea plants using XFM.

Supplemental Figure S3. Changes in Mn concentration in leaf tissues of cowpea scanned repeatedly over 48 h.

Supplemental Figure S4. XFM images showing the distribution of Ca in a portion of a leaf of cowpea exposed to 30 μM Mn.

Supplemental Movie S1. Microtomography used to examine elemental distribution within an intact leaf of spinifex.

ACKNOWLEDGMENTS

The assistance of Cui Li (University of Queensland) in conducting the analyses of the foliar-applied fertilizers is acknowledged. We thank Nathan Reid (Commonwealth Scientific and Industrial Research Organization, Australia) and Martin de Jonge (Australian Synchrotron) for providing the microtomography data for the spinifex leaf.

Received June 21, 2018; accepted August 7, 2018; published August 14, 2018.

OUTSTANDING QUESTIONS

- Is it possible to effectively use XFM analyses as a high-throughput, non-destructive screening method in molecular biology?
- Can XFM analyses be used to provide simultaneous analyses of nutrient distribution and protein (transporter) localization by using exotic metal tags?
- Can the recent development of repeated (kinetic) in vivo analyses of multi-element distribution in plant tissue be used to provide further information across the broad range of studies in plant sciences, including for functional characterization in molecular biology?
- Will the development of XANES imaging and tomography in living plants now enable new areas of study in plant sciences, such as screening for differences in elemental speciation between phenotypes?

LITERATURE CITED

Ajiboye B, Cakmak I, Paterson D, de Jonge MD, Howard DL, Stacey SP, Torun AA, Aydin N, McLaughlin MJ (2015) X-ray fluorescence microscopy of zinc localization in wheat grains biofortified through foliar zinc applications at different growth stages under field conditions. Plant Soil **392**: 357–370

Beetz T, Jacobsen C (2003) Soft X-ray radiation-damage studies in PMMA using a cryo-STXM. J Synchrotron Radiat **10**: 280–283

Berglund A, Brelid H, Rindby A, Engström P (1999) Spatial distribution of metal ions in spruce wood by synchrotron radiation microbeam X-ray fluorescence analysis. Holzforschung **53**: 474

Bertsch PM, Hunter DB (2001) Applications of synchrotron-based X-ray microprobes. Chem Rev **101**: 1809–1842

Blamey FPC, Hernandez-Soriano MC, Cheng M, Tang C, Paterson DJ, Lombi E, Wang WH, Scheckel KG, Kopittke PM (2015) Synchrotron-based techniques shed light on mechanisms of plant sensitivity and tolerance to high manganese in the root environment. Plant Physiol **169**: 2006–2020

Blamey FPC, McKenna BA, Li C, Cheng M, Tang C, Jiang H, Howard DL, Paterson DJ, Kappen P, Wang P, (2018a) Manganese distribution and speciation help to explain the effects of silicate and phosphate on manganese toxicity in four crop species. New Phytol **217**: 1146–1160

Blamey FPC, Paterson DJ, Walsh A, Afshar N, McKenna BA, Cheng M, Tang C, Horst WJ, Menzies NW, Kopittke PM (2018b) Time-resolved analyses of elemental distribution and concentration in living plants: an example using Mn toxicity in cowpea leaves. Ann Bot (Lond) **156**: 151–160

Bulska E, Wysocka IA, Wierzbicka ML, Proost K, Janssens K, Falkenberg G (2006) In vivo investigation of the distribution and the local speciation of selenium in *Allium cepa* L. by means of microscopic X-ray absorption near-edge structure spectroscopy and confocal microscopic X-ray fluorescence analysis. Anal Chem **78**: 7616–7624

Castillo-Michel HA, Larue C, Pradas Del Real AE, Cotte M, Sarret G (2017) Practical review on the use of synchrotron based micro- and nano-X-ray fluorescence mapping and X-ray absorption spectroscopy to investigate the interactions between plants and engineered nanomaterials. Plant Physiol Biochem **110**: 13–32

Caulfield L, Black R (2004) Zinc deficiency. *In* **M Ezzati, DL Lopez, A Rodgers, CJL Murray**, eds, Comparative Quantification of Health Risks: Global and Regional Burden of Disease Attribution to Selected Major Risk Factors. World Health Organization, Geneva, pp 257–279

Chao DY, Chen Y, Chen J, Shi S, Chen Z, Wang C, Danku JM, Zhao FJ, Salt DE (2014) Genome-wide association mapping identifies a new arsenate reductase enzyme critical for limiting arsenic accumulation in plants. PLoS Biol **12**: e1002009

Chen S, Deng J, Yuan Y, Flachenecker C, Mak R, Hornberger B, Jin Q, Shu D, Lai B, Maser J, (2014) The Bionanoprobe: hard X-ray fluorescence nanoprobe with cryogenic capabilities. J Synchrotron Radiat **21**: 66–75

Chu HH, Car S, Socha AL, Hindt MN, Punshon T, Guerinot ML (2017) The Arabidopsis MTP8 transporter determines the localization of manganese and iron in seeds. Sci Rep **7**: 11024

Conte SS, Chu HH, Rodriguez DC, Punshon T, Vasques KA, Salt DE, Walker EL (2013) *Arabidopsis thaliana* Yellow Stripe1-Like4 and Yellow Stripe1-Like6 localize to internal cellular membranes and are involved in metal ion homeostasis. Front Plant Sci **4**: 283

Datta R, Das P, Tappero R, Punamiya P, Elzinga E, Sahi S, Feng H, Kiiskila J, Sarkar D (2017) Evidence for exocellular arsenic in fronds of *Pteris vittata*. Sci Rep **7**: 2839

De Brier N, Gomand SV, Donner E, Paterson D, Delcour JA, Lombi E, Smolders E (2015) Distribution of minerals in wheat grains (*Triticum aestivum* L.) and in roller milling fractions affected by pearling. J Agric Food Chem **63**: 1276–1285

De Brier N, Gomand SV, Donner E, Paterson D, Smolders E, Delcour JA, Lombi E (2016) Element distribution and iron speciation in mature wheat grains (*Triticum aestivum* L.) using synchrotron X-ray fluorescence microscopy mapping and X-ray absorption near-edge structure (XANES) imaging. Plant Cell Environ **39**: 1835–1847

de Jonge MD, Holzner C, Baines SB, Twining BS, Ignatyev K, Diaz J, Howard DL, Legnini D, Miceli A, McNulty I, (2010) Quantitative 3D elemental microtomography of *Cyclotella meneghiniana* at 400-nm resolution. Proc Natl Acad Sci USA **107**: 15676–15680

Donner E, Punshon T, Guerinot ML, Lombi E (2012) Functional characterisation of metal(loid) processes in planta through the integration of synchrotron techniques and plant molecular biology. Anal Bioanal Chem **402**: 3287–3298

Doolette CL, Read TL, Li C, Scheckel KG, Donner E, Kopittke PM, Schjoerring JK, Lombi E (2018) Foliar application of zinc sulphate and zinc EDTA to wheat leaves: differences in mobility, distribution, and speciation. J Exp Bot **69**: 4469–4481

Du Y, Kopittke PM, Noller BN, James SA, Harris HH, Xu ZP, Li P, Mulligan DR, Huang L (2015) *In situ* analysis of foliar zinc absorption and short-distance movement in fresh and hydrated leaves of tomato and citrus using synchrotron-based X-ray fluorescence microscopy. Ann Bot **115**: 41–53

Eroglu S, Giehl RFH, Meier B, Takahashi M, Terada Y, Ignatyev K, Andresen E, Küpper H, Peiter E, von Wirén N (2017) Metal Tolerance Protein 8 mediates manganese homeostasis and iron reallocation during seed development and germination. Plant Physiol **174**: 1633–1647

Fernández V, Brown PH (2013) From plant surface to plant metabolism: the uncertain fate of foliar-applied nutrients. Front Plant Sci **4**: 289

Fittschen UEA, Kunz HH, Höhner R, Tyssebotn IMB, Fittschen A (2017) A new micro X-ray fluorescence spectrometer for *in vivo* elemental analysis in plants. X-Ray Spectrom **46**: 374–381

Freeman JL, Zhang LH, Marcus MA, Fakra S, McGrath SP, Pilon-Smits EAH (2006) Spatial imaging, speciation, and quantification of selenium in the hyperaccumulator plants *Astragalus bisulcatus* and *Stanleya pinnata*. Plant Physiol **142**: 124–134

Fukumoto N, Kobayashi Y, Kurahashi M, Kojima I (1999) X-ray fluorescent spectroscopy with a focused X-ray beam collimated by a glass capillary guide tube and element mapping of biological samples. Spectrochim Acta B Atomic Spectrosc **54**: 91–98

Gei V, Erskine PD, Harris HH, Echevarria G, Mesjasz-Przybyłowicz J, Barnabas AD, Przybyłowicz WJ, Kopittke PM, van der Ent A (2018) Tools for the discovery of hyperaccumulator plant species and understanding their ecophysiology. *In* **A Van der Ent, G Echevarria, AJM Baker, JL Morel**, eds, Agromining: Farming for Metals: Extracting Unconventional Resources Using Plants. Springer International Publishing, Cham, Switzerland, pp 117–133

Giesen C, Wang HAO, Schapiro D, Zivanovic N, Jacobs A, Hattendorf B, Schüffler PJ, Grolimund D, Buhmann JM, Brandt S, (2014) Highly multiplexed imaging of tumor tissues with subcellular resolution by mass cytometry. Nat Methods **11**: 417–422

Gilfrich JV, Gilfrich NL, Skelton EF, Kirkland JP, Qadri SB, Nagel DJ (1991) X-ray fluorescence analysis of tree rings. X-Ray Spectrom **20**: 203–208

Hernandez-Viezcas JA, Castillo-Michel H, Andrews JC, Cotte M, Rico C, Peralta-Videa JR, Ge Y, Priester JH, Holden PA, Gardea-Torresdey JL

(2013) In situ synchrotron X-ray fluorescence mapping and speciation of CeO_2 and ZnO nanoparticles in soil cultivated soybean (Glycine max). ACS Nano **7**: 1415–1423

Isaure MP, Huguet S, Meyer CL, Castillo-Michel H, Testemale D, Vantelon D, Saumitou-Laprade P, Verbruggen N, Sarret G (2015) Evidence of various mechanisms of Cd sequestration in the hyperaccumulator *Arabidopsis halleri*, the non-accumulator *Arabidopsis lyrata*, and their progenies by combined synchrotron-based techniques. J Exp Bot **66**: 3201–3214

Johnson AAT, Kyriacou B, Callahan DL, Carruthers L, Stangoulis J, Lombi E, Tester M (2011) Constitutive overexpression of the OsNAS gene family reveals single-gene strategies for effective iron- and zinc-biofortification of rice endosperm. PLoS ONE **6**: e24476

Kim SA, Punshon T, Lanzirotti A, Li L, Alonso JM, Ecker JR, Kaplan J, Guerinot ML (2006) Localization of iron in Arabidopsis seed requires the vacuolar membrane transporter VIT1. Science **314**: 1295–1298

Kopittke PM, Menzies NW, de Jonge MD, McKenna BA, Donner E, Webb RI, Paterson DJ, Howard DL, Ryan CG, Glover CJ, (2011) In situ distribution and speciation of toxic copper, nickel, and zinc in hydrated roots of cowpea. Plant Physiol **156**: 663–673

Kopittke PM, de Jonge MD, Menzies NW, Wang P, Donner E, McKenna BA, Paterson D, Howard DL, Lombi E (2012) Examination of the distribution of arsenic in hydrated and fresh cowpea roots using two- and three-dimensional techniques. Plant Physiol **159**: 1149–1158

Kopittke PM, Lombi E, McKenna BA, Wang P, Donner E, Webb RI, Blamey FPC, de Jonge MD, Paterson D, Howard DL, (2013) Distribution and speciation of Mn in hydrated roots of cowpea at levels inhibiting root growth. Physiol Plant **147**: 453–464

Kopittke PM, de Jonge MD, Wang P, McKenna BA, Lombi E, Paterson DJ, Howard DL, James SA, Spiers KM, Ryan CG, (2014) Laterally resolved speciation of arsenic in roots of wheat and rice using fluorescence-XANES imaging. New Phytol **201**: 1251–1262

Kyriacou B, Moore KL, Paterson D, de Jonge MD, Howard DL, Stangoulis J, Tester M, Lombi E, Johnson AAT (2014) Localization of iron in rice grain using synchrotron X-ray fluorescence microscopy and high resolution secondary ion mass spectrometry. J Cereal Sci **59**: 173–180

Larue C, Castillo-Michel H, Stein RJ, Fayard B, Pouyet E, Villanova J, Magnin V, Pradas del Real AE, Trcera N, Legros S, (2016) Innovative combination of spectroscopic techniques to reveal nanoparticle fate in a crop plant. Spectrochim Acta B Atomic Spectrosc **119**: 17–24

Levenson RM, Borowsky AD, Angelo M (2015) Immunohistochemistry and mass spectrometry for highly multiplexed cellular molecular imaging. Lab Invest **95**: 397–405

Li C, Wang P, Menzies NW, Lombi E, Kopittke PM (2017) Effects of changes in leaf properties mediated by methyl jasmonate (MeJA) on foliar absorption of Zn, Mn and Fe. Ann Bot **120**: 405–415

Li C, Wang P, Lombi E, Cheng M, Tang C, Howard DL, Menzies NW, Kopittke PM (2018a) Absorption of foliar-applied Zn fertilizers by trichomes in soybean and tomato. J Exp Bot **69**: 2717–2729

Li C, Wang P, Van der Ent A, Cheng M, Jiang H, Lombi E, Tang C, De Jonge MD, Menzies NW, Kopittke PM (2018b) Absorption and translocation of foliar-applied ZnSO4 and nano-ZnO in sunflower (Helianthus annuus): importance of the cuticle, stomata and trichomes. Ann Bot (Lond) **69**: 2717–2729

Lombi E, Susini J (2009) Synchrotron-based techniques for plant and soil science: opportunities, challenges and future perspectives. Plant Soil **320**: 1–35

Lombi E, Scheckel KG, Pallon J, Carey AM, Zhu YG, Meharg AA (2009) Speciation and distribution of arsenic and localization of nutrients in rice grains. New Phytol **184**: 193–201

Lombi E, de Jonge MD, Donner E, Kopittke PM, Howard DL, Kirkham R, Ryan CG, Paterson D (2011a) Fast X-ray fluorescence microtomography of hydrated biological samples. PLoS ONE6: e20626

Lombi E, Scheckel KG, Kempson IM (2011b) In situ analysis of metal(loid)s in plants: state of the art and artefacts. Environ Exp Bot **72**: 3–17

Lombi E, Smith E, Hansen TH, Paterson D, de Jonge MD, Howard DL, Persson DP, Husted S, Ryan C, Schjoerring JK (2011c) Megapixel imaging of (micro)nutrients in mature barley grains. J Exp Bot **62**: 273–282

Lu L, Liao X, Labavitch J, Yang X, Nelson E, Du Y, Brown PH, Tian S (2014) Speciation and localization of Zn in the hyperaccumulator *Sedum alfredii* by extended X-ray absorption fine structure and micro-X-ray fluorescence. Plant Physiol Biochem **84**: 224–232

Lu L, Xie R, Liu T, Wang H, Hou D, Du Y, He Z, Yang X, Sun H, Tian S (2017) Spatial imaging and speciation of Cu in rice (*Oryza sativa* L.) roots using synchrotron-based X-ray microfluorescence and X-ray absorption spectroscopy. Chemosphere **175**: 356–364

Ma Y, He X, Zhang P, Zhang Z, Ding Y, Zhang J, Wang G, Xie C, Luo W, Zhang J, (2017) Xylem and phloem based transport of CeO_2 nanoparticles in hydroponic cucumber plants. Environ Sci Technol **51**: 5215–5221

Martínez-Criado G, Villanova J, Tucoulou R, Salomon D, Suuronen JP, Labouré S, Guilloud C, Valls V, Barrett R, Gagliardini E, (2016) ID16B: a hard X-ray nanoprobe beamline at the ESRF for nano-analysis. J Synchrotron Radiat **23**: 344–352

McNear DH Jr, Peltier E, Everhart J, Chaney RL, Sutton S, Newville M, Rivers M, Sparks DL (2005) Application of quantitative fluorescence and absorption-edge computed microtomography to image metal compartmentalization in *Alyssum murale*. Environ Sci Technol **39**: 2210–2218

Meharg AA, Lombi E, Williams PN, Scheckel KG, Feldmann J, Raab A, Zhu Y, Islam R (2008) Speciation and localization of arsenic in white and brown rice grains. Environ Sci Technol **42**: 1051–1057

Melkonian S, Argos M, Hall MN, Chen Y, Parvez F, Pierce B, Cao H, Aschebrook-Kilfoy B, Ahmed A, Islam T, (2013) Urinary and dietary analysis of 18,470 Bangladeshis reveal a correlation of rice consumption with arsenic exposure and toxicity. PLoS ONE **8**: e80691

Mitter N, Worrall EA, Robinson KE, Li P, Jain RG, Taochy C, Fletcher SJ, Carroll BJ, Lu GQ, Xu ZP (2017) Clay nanosheets for topical delivery of RNAi for sustained protection against plant viruses. Nat Plants **3**: 16207

Myers SS, Zanobetti A, Kloog I, Huybers P, Leakey ADB, Bloom AJ, Carlisle E, Dietterich LH, Fitzgerald G, Hasegawa T, (2014) Increasing CO_2 threatens human nutrition. Nature **510**: 139–142

Neal AL, Geraki K, Borg S, Quinn P, Mosselmans JF, Brinch-Pedersen H, Shewry PR (2013) Iron and zinc complexation in wild-type and ferritin-expressing wheat grain: implications for mineral transport into developing grain. J Biol Inorg Chem **18**: 557–570

Oli P, Ward R, Adhikari B, Mawson AJ, Adhikari R, Wess T, Pallas L, Spiers K, Paterson D, Torley P (2016) Synchrotron X-ray fluorescence microscopy study of the diffusion of iron, manganese, potassium and zinc in parboiled rice kernels. Lebensm Wiss Technol **71**: 138–148

Pickering IJ, Prince RC, Salt DE, George GN (2000) Quantitative, chemically specific imaging of selenium transformation in plants. Proc Natl Acad Sci USA **97**: 10717–10722

Pickering IJ, Gumaelius L, Harris HH, Prince RC, Hirsch G, Banks JA, Salt DE, George GN (2006) Localizing the biochemical transformations of arsenate in a hyperaccumulating fern. Environ Sci Technol **40**: 5010–5014

Punshon T, Guerinot ML, Lanzirotti A (2009) Using synchrotron X-ray fluorescence microprobes in the study of metal homeostasis in plants. Ann Bot **103**: 665–672

Punshon T, Hirschi K, Yang J, Lanzirotti A, Lai B, Guerinot ML (2012) The role of CAX1 and CAX3 in elemental distribution and abundance in Arabidopsis seed. Plant Physiol **158**: 352–362

Punshon T, Tappero R, Ricachenevsky FK, Hirschi K, Nakata PA (2013) Contrasting calcium localization and speciation in leaves of the Medicago truncatula mutant *cod5* analyzed via synchrotron X-ray techniques. Plant J **76**: 627–633

Ramos I, Pataco IM, Mourinho MP, Lidon F, Reboredo F, Pessoa MF, Carvalho ML, Santos JP, Guerra M (2016) Elemental mapping of biofortified wheat grains using micro X-ray fluorescence. Spectrochim Acta B Atomic Spectrosc **120**: 30–36

Reeves RD, Baker AJM, Jaffré T, Erskine PD, Echevarria G, van der Ent A (2018) A global database for plants that hyperaccumulate metal and metalloid trace elements. New Phytol **218**: 407–411

Ryan CG, Kirkham R, Hough RM, Moorhead G, Siddons DP, de Jonge MD, Paterson DJ, De Geronimo G, Howard DL, Cleverley JS (2010) Elemental X-ray imaging using the Maia detector array: the benefits and challenges of large solid-angle. Nucl Instrum Methods Phys Res A **619**: 37–43

Sarret G, Schroeder WH, Marcus MA, Geoffroy N, Manceau A (2003) Localization and speciation of Zn in mycorrhized roots by μSXRF and μEXAFS. J Phys IV **107**: 1193–1196

Scheckel KG, Lombi E, Rock SA, McLaughlin MJ (2004) In vivo synchrotron study of thallium speciation and compartmentation in *Iberis intermedia*. Environ Sci Technol **38**: 5095–5100

Scheckel KG, Hamon R, Jassogne L, Rivers M, Lombi E (2007) Synchrotron X-ray absorption-edge computed microtomography imaging of thallium compartmentalization in *Iberis intermedia*. Plant Soil **290**: 51–60

Schulze DG, Bertsch PM (1995) Synchrotron X-ray techniques in soil, plant, and environmental research. Adv Agron **55**: 1–66

Servin AD, Castillo-Michel H, Hernandez-Viezcas JA, Diaz BC, Peralta-Videa JR, Gardea-Torresdey JL (2012) Synchrotron micro-XRF and micro-XANES confirmation of the uptake and translocation of TiO_2 nanoparticles in cucumber (Cucumis sativus) plants. Environ Sci Technol **46**: 7637–7643

Song Y, Wang Y, Mao W, Sui H, Yong L, Yang D, Jiang D, Zhang L, Gong Y (2017) Dietary cadmium exposure assessment among the Chinese population. PLoS ONE **12**: e0177978

Spielman-Sun E, Lombi E, Donner E, Howard D, Unrine JM, Lowry GV (2017) Impact of surface charge on cerium oxide nanoparticle uptake and translocation by wheat (*Triticum aestivum*). Environ Sci Technol **51**: 7361–7368

Takahashi M, Nozoye T, Kitajima N, Fukuda N, Hokura A, Terada Y, Nakai I, Ishimaru Y, Kobayashi T, Nakanishi HK, (2009) In vivo analysis of metal distribution and expression of metal transporters in rice seed during germination process by microarray and X-ray fluorescence imaging of Fe, Zn, Mn, and Cu. Plant Soil **325**: 39

Tappero R, Peltier E, Gräfe M, Heidel K, Ginder-Vogel M, Livi KJT, Rivers ML, Marcus MA, Chaney RL, Sparks DL (2007) Hyperaccumulator *Alyssum murale* relies on a different metal storage mechanism for cobalt than for nickel. New Phytol **175**: 641–654

Terzano R, Al Chami Z, Vekemans B, Janssens K, Miano T, Ruggiero P (2008) Zinc distribution and speciation within rocket plants (*Eruca vesicaria* L. Cavalieri) grown on a polluted soil amended with compost as determined by XRF microtomography and micro-XANES. J Agric Food Chem **56**: 3222–3231

Terzano R, Alfeld M, Janssens K, Vekemans B, Schoonjans T, Vincze L, Tomasi N, Pinton R, Cesco S (2013) Spatially resolved (semi)quantitative determination of iron (Fe) in plants by means of synchrotron micro X-ray fluorescence. Anal Bioanal Chem **405**: 3341–3350

Tian S, Lu L, Yang X, Webb SM, Du Y, Brown PH (2010) Spatial imaging and speciation of lead in the accumulator plant *Sedum alfredii* by microscopically focused synchrotron X-ray investigation. Environ Sci Technol **44**: 5920–5926

Tian S, Lu L, Labavitch J, Yang X, He Z, Hu H, Sarangi R, Newville M, Commisso J, Brown P (2011) Cellular sequestration of cadmium in the hyperaccumulator plant species *Sedum alfredii*. Plant Physiol **157**: 1914–1925

Tian S, Lu L, Xie R, Zhang M, Jernstedt JA, Hou D, Ramsier C, Brown PH (2015) Supplemental macronutrients and microbial fermentation products improve the uptake and transport of foliar applied zinc in sunflower (*Helianthus annuus* L.) plants: studies utilizing micro X-ray florescence. Front Plant Sci **5**: 808

Tolrà R, Vogel-Mikuš K, Hajiboland R, Kump P, Pongrac P, Kaulich B, Gianoncelli A, Babin V, Barceló J, Regvar M, (2011) Localization of aluminium in tea (*Camellia sinensis*) leaves using low energy X-ray fluorescence spectro-microscopy. J Plant Res **124**: 165–172

Valdez Barillas JR, Quinn CF, Freeman JL, Lindblom SD, Fakra SC, Marcus MA, Gilligan TM, Alford ÉR, Wangeline AL, Pilon-Smits EAH (2012) Selenium distribution and speciation in the hyperaccumulator *Astragalus bisulcatus* and associated ecological partners. Plant Physiol **159**: 1834–1844

van der Ent A, Przybyłowicz WJ, de Jonge MD, Harris HH, Ryan CG, Tylko G, Paterson DJ, Barnabas AD, Kopittke PM, Mesjasz-Przybyłowicz J (2018) X-ray elemental mapping techniques for elucidating the ecophysiology of hyperaccumulator plants. New Phytol **218**: 432–452

Wang L, Zhang T, Li P, Huang W, Tang J, Wang P, Liu J, Yuan Q, Bai R, Li B, (2015a) Use of synchrotron radiation-analytical techniques to reveal chemical origin of silver-nanoparticle cytotoxicity. ACS Nano **9**: 6532–6547

Wang P, Menzies NW, Lombi E, McKenna BA, de Jonge MD, Paterson DJ, Howard DL, Glover CJ, James S, Kappen P, (2013a) *In situ* speciation and distribution of toxic selenium in hydrated roots of cowpea. Plant Physiol **163**: 407–418

Wang P, Menzies NW, Lombi E, McKenna BA, Johannessen B, Glover CJ, Kappen P, Kopittke PM (2013b) Fate of ZnO nanoparticles in soils and cowpea (*Vigna unguiculata*). Environ Sci Technol **47**: 13822–13830

Wang P, Menzies NW, Lombi E, McKenna BA, James S, Tang C, Kopittke PM (2015b) Synchrotron-based X-ray absorption near-edge spectroscopy imaging for laterally resolved speciation of selenium in fresh roots and leaves of wheat and rice. J Exp Bot **66**: 4795–4806

Wang P, Lombi E, Zhao FJ, Kopittke PM (2016) Nanotechnology: a new opportunity in plant sciences. Trends Plant Sci **21**: 699–712

Wang P, Lombi E, Sun S, Scheckel KG, Malysheva A, McKenna BA, Menzies NW, Zhao FJ, Kopittke PM (2017) Characterizing the uptake, accumulation and toxicity of silver sulfide nanoparticles in plants. Environ Sci Nano **4**: 448–460

Werker E (2000) Trichome diversity and development. Adv Bot Res **31**: 1–35

WHO (2007) Assessing the Iron Status of Populations. World Health Organization, Geneva, p 108

Yamaoka W, Takada S, Takehisa H, Hayashi Y, Hokura A, Terada Y, Abe T, Nakai I (2010) Study on accumulation mechanism of cadmium in rice (*Oriza sativa* L.) by micro-XRF imaging and X-ray absorption fine structure analysis utilizing synchrotron radiation. Bunseki Kagaku **59**: 463–475

Young LW, Westcott ND, Attenkofer K, Reaney MJT (2006) A high-throughput determination of metal concentrations in whole intact *Arabidopsis thaliana* seeds using synchrotron-based X-ray fluorescence spectroscopy. J Synchrotron Radiat **13**: 304–313

Yun W, Pratt ST, Miller RM, Cai Z, Hunter DB, Jarstfer AG, Kemner KM, Lai B, Lee HR, Legnini DG, (1998) X-ray imaging and microspectroscopy of plants and fungi. J Synchrotron Radiat **5**: 1390–1395

Zhai Z, Gayomba SR, Jung HI, Vimalakumari NK, Piñeros M, Craft E, Rutzke MA, Danku J, Lahner B, Punshon T, (2014) OPT3 is a phloem-specific iron transporter that is essential for systemic iron signaling and redistribution of iron and cadmium in *Arabidopsis*. Plant Cell **26**: 2249–2264

Zhang T, Sun H, Lv Z, Cui L, Mao H, Kopittke PM (2018) Using synchrotron-based approaches to examine the foliar application of $ZnSO_4$ and ZnO nanoparticles for field-grown winter wheat. J Agric Food Chem **66**: 2572–2579

Zhao FJ, Moore KL, Lombi E, Zhu YG (2014) Imaging element distribution and speciation in plant cells. Trends Plant Sci **19**: 183–192

Zhao L, Sun Y, Hernandez-Viezcas JA, Hong J, Majumdar S, Niu G, Duarte-Gardea M, Peralta-Videa JR, Gardea-Torresdey JL (2015) Monitoring the environmental effects of CeO_2 and ZnO nanoparticles through the life cycle of corn (*Zea mays*) plants and *in situ* μ-XRF mapping of nutrients in kernels. Environ Sci Technol **49**: 2921–2928